Isolated Polymer Chains via Mixed Self-Assembled Monolayers: Morphology and Friction Studied by Scanning Force Microscopy

V. Koutsos, E. W. van der Vegte, P. C. M. Grim,† and G. Hadziioannou*

Department of Polymer Chemistry and Materials Science Centre, University of Groningen, Nijenborgh 4, 9747 AG Groningen, The Netherlands

Received May 5, 1997; Revised Manuscript Received October 9, 1997[⊗]

ABSTRACT: In this paper, we describe a system of mixed self-assembled monolayers of alkanethiols and thiol-terminated polystyrene (PS-SH) chemisorbed on a gold surface from mixed toluene solutions. Topography and friction images were obtained with a scanning force microscope (SFM) under bad-solvent conditions. We observed randomly distributed single polystyrene coils. We found that the polymer grafting density increases when the molar ratio of polymer to alkanethiol in solution increases. The local friction coefficient on a collapsed polystyrene chain was found to be about 0.3, a value that compares with a macroscopic one of 0.515. X-ray photoelectron spectroscopy and ellipsometry were employed to verify and supplement the SFM measurements.

1. Introduction

The modification of surfaces by end-grafted polymer chains is of great practical interest in steric stabilization of colloidal suspensions[1] adhesion,[2,3] and friction.[4,5] Densely grafted polymer chains under good-solvent conditions stretch away from the surface, forming a "brush",[6] while under bad-solvent conditions they collapse collectively onto the surface, forming either a uniform layer or well-defined clusters.[7−9] Self-assembling monolayers (SAM's) of short molecules have also proven to be useful for surface modification since they affect the above-mentioned macroscopic surface properties.[10] Recently, SAM's derived from organic sulfur compounds have been extensively studied.[11−21] Organic thiols chemisorb onto gold surfaces forming a densely packed, crystalline-like structure in which the alkyl chains are slightly tilted with respect to the surface normal. The thiol head group is believed to bind covalently to the gold surface through a gold thiolate bond. The functional tail group is exposed to the free surface. So far, most of the work with these SAM's has been carried out with suitable alkanethiols,[22−25] dialkyl sulfides, and dialkyl disulfides;[26,27] few studies dealt with thiol-terminated polymers.[28−31] The tail group as well as the length of the alkyl chains has been varied in order to obtain the desired properties. The use of mixed SAM's allows even more control over physical and chemical properties of solid surfaces.[15,16]

In this paper we present the preparation of mixed monolayers of alkanethiols and PS-SH on gold surfaces from two-component solutions and their imaging under bad-solvent conditions using scanning force microscopy (SFM). We acquired both topography and lateral force images.

Force modulation measurements were published in the past.[34]

Imaging of polymer layers using SFM in the strong segregation limit (bad-solvent conditions) has been proven to be quite successful[9,32,33] due to the strong polymer−polymer interaction which results in an increased structural stability of the layers. The grafting density of the monolayer is not affected by the change of the solvent since the chemisorbed molecules are irreversibly grafted onto the gold substrate. We found that when a gold substrate is brought into contact with a solution containing a mixture of short alkanethiols and PS-SH a mixed monolayer is spontaneously formed within which single polymer chains are randomly distributed. By varying the relative concentrations of the two components in the solution, the grafting density of the chains can be changed. To our knowledge this is the first system which allows covalent end-grafting of polymers with good control over the grafting density in the mushroom regime.

2. Experimental Section

2.1. Materials. Dodecanethiol (Janssen Chimica) and toluene p.a. (Merck) were used as received. Styrene (Janssen Chimica) was distilled from calcium hydride at reduced pressure (15 mbar) and stored under nitrogen at −20 °C. Styrene was distilled from dibutylmagnesium at reduced pressure (15 mbar) just prior to use. Tetrahydrofuran (THF, Janssen Chimica), used as a solvent, was dried by Na/benzophenone under argon. It was refluxed until a deep purple color was obtained, indicating dryness, and then collected under argon. Propylene sulfide (Aldrich) was distilled from calcium hydride under argon and stored under argon at −20 °C. Cumylpotassium carbanion was used as a monofunctional initiator.[35] A 0.1 M solution of this initiator was prepared by adding 0.4 g of potassium and 1.4 mL of bis(α-methylbenzyl)ether to 50 mL of dry THF at −20 °C under argon. The colourless solution slowly darkened to deep red. After warming to room temperature, the solution was stirred overnight. Gold wire (Schöne Edelmetalen) was 99.99% pure.

2.2. Synthesis of Thiol-Terminated Polystyrene. Thiol-terminated polystyrene (PS-SH) was prepared by anionic polymerization.[29,35] A 250 mL Schlenk tube was filled with 150 mL of dry THF under argon. A sufficient amount of initiator was added to the THF to maintain a pink color while the solvent was cooled to −78 °C by a methanol/acetone bath. This method was used to deactivate impurities which could cause premature termination of the living chains. The appropriate amount of initiator for the desired molecular weight was added at once, 10 mL of styrene was added dropwise. At

* To whom correspondence should be addressed.
† Present address: University of Leuven (KUL), Department of Chemistry, Laboratory of Molecular Dynamics and Spectroscopy, Celestijnenlaan 200-F, 3001 Heverlee, Belgium.
⊗ Abstract published in *Advance ACS Abstracts,* December 15, 1997.

S0024-9297(97)00618-9 CCC: $15.00
Published on Web 01/13/1998

Table 1. PS_x-SH[a] Characteristics

polymer	M_w	M_w/M_n	R_f (nm)
PS_{400}-SH	41 500	1.09	16.1
PS_{1400}-SH	144 000	1.2	33.3
PS_{2500}-SH	258 000	1.1	46.9

[a] The subscript refers to the approximate degree of polymerization.

the end of the styrene polymerization reaction the solution was still red, indicating the presence of living chain ends. The polystyryl anions were titrated with propylene sulfide and subsequently protonated with acidic methanol to obtain the thiol-terminated polystyrene (the solution becomes colourless). The polymer was isolated by precipitation in methanol and further purified by repeated dissolution in THF and precipitation in methanol. The molecular weight and the molecular weight distribution of the polymer were determined by gel permeation chromatography (GPC) using a Spectra Physics system with a Spectra Physics AS1000 autosampler, PLgel 5 μm mixed column, a Shodex RI71 refractive index detector, and a Viscotec H502 viscometer detector. Molecular weight data for all PS_x-SH are given in Table 1.

2.3. Substrate Gold Film Preparation. Mica was cleaved in air and immediately placed in the vacuum chamber of a diffusion-pumped thermal evaporator (Edwards Auto 306). The mica sheets were heated to 400 °C at a pressure below 1×10^{-4} mbar. Gold was evaporated from resistively heated tungsten boats at a pressure below 5×10^{-6} mbar. The thickness of the gold layer was monitored with a quartz crystal oscillator and eventually amounted to 40 nm (deposition rate 3 nm/min). The gold substrates were left at 400 °C for 2 h and then cooled down to room temperature in vacuum. The vacuum chamber was backfilled with prepurified nitrogen and the gold substrates were removed and stored under nitrogen until further use.

2.4. Monolayer Preparation and Characterization. All the samples were prepared by exposing the gold substrates to two-component solutions of PS-SH and dodecanethiol in toluene of the desired composition. The PS-SH concentration in the solution was kept well below the critical overlap concentration c^*.[36] The adsorption solutions of the desired mole fraction PS-SH (ϕ_{PS-SH}) were prepared by keeping the PS-SH concentration constant and adding the appropriate amount of dodecanethiol. Here ϕ_{PS-SH} equals the ratio of the number of moles of PS-SH (n_{PS-SH}) and the total number of moles of the two adsorbing components ($n_{PS-SH} + n_{dodecanethiol}$) in the solution:

$$\phi_{PS-SH} = \frac{n_{PS-SH}}{n_{PS-SH} + n_{dodecanethiol}} \quad (1)$$

In the case of PS_{400}-SH, we used a concentration of 2 mg/mL, and for PS_{1400}-SH and PS_{2500}-SH we used 1 mg/mL. After 48 h the substrates were removed from the adsorption solution and immediately rinsed exhaustively with neat toluene. The samples were dried under a stream of argon, placed in a vacuum at 50 °C for 1 h, and stored in nitrogen. The monolayers were characterized by X-ray photoelectron spectroscopy (XPS) using a Surface Science SSX-100 spectrometer with Mg Kα excitation, a concentric hemispherical analyzer, and multichannel detector. The carbon-1s (C_{1s}) signal was normalized with respect to the Au_{4f} signal. Monolayer thicknesses were measured using a home-built ellipsometer with a wavelength of 632.8 nm. Freshly prepared bare gold was used as a reference. Thicknesses were calculated assuming a refractive index of 1.59 for the monolayer. All measurements were done under bad-solvent conditions for PS (vacuum for XPS and air for ellipsometry). Flory radii of gyration of the polymer chains in solution were measured by light scattering using a DAWN DSP-F instrument, at a wavelength of 632.8 nm (Table 1). XPS measurements and SFM images indicate no adsorption of unmodified polystyrene from a toluene solution onto a gold surface. It has been demonstrated that the adsorption process of modified polystyrene PS-SH (in polymer-only solutions) is complete after 48 h when a polymer concentration of 2 mg/mL or smaller is used.[29] The characteristic chemisorption time for the alkanethiol solutions (for concentrations of about 5 μM) is on the order of some minutes.[37]

2.5. Scanning Force Microscopy. The scanning force microscopy[38] experiments have been performed either under ambient conditions using a Park Scientific Instrument or under water (bad solvent for PS molecules) using a Topometrix AFM (Explorer). Imaging was performed in the contact mode (tip in contact with the surface) with the applied force kept constant. For the measurements in air we used the attractive regime (cantilever bent toward the surface). This was done by operating at a cantilever deflection a little smaller than that at which the tip loses contact with the surface. In ambient conditions, it was very difficult to image the coils in the repulsive regime. In water the imaging process was easier. Within the range of about 1−5 nN, reproducible and similar images were taken. The adhesive force was determined from force−distance curves to be around 2 nN. During attempts to image the monolayer with a negative applied force (applied force ≈ adhesive force) the tip usually snapped up out of contact after a few line scans. In addition to topography images, lateral force images were obtained. While the sample is scanned perpendicular to the long axis of the cantilever, the output of the horizontal two quadrants of the photodiode detector is measured. In this configuration, the lateral force will cause the cantilever to twist. The degree of twisting can be monitored from the differential signal between the left and right detector and it can be related to the magnitude of the total lateral force. Commercially available SiO_2 (V-shaped, force constant 0.03 N/m) and Si_3N_4 (V-shaped, force constants 0.032 and 0.1 N/m) cantilevers were used. The scanning speeds used were in the range of 5 μm/s. All SFM results displayed excellent reproducibility, and the measurements that are presented here are typical. The images are shown without any processing except leveling.

2.6. Measuring the Tip Radius and Deconvolution. In Figure 1a an image of the bare gold substrate is presented. Individual, atomically flat Au terraces separated by steps and deep channels (dark areas) can be observed. Zheng et al.[39] have shown, using SEM at large incident angle (50°), that the sides of the gold islands are sharp and nearly vertical. The sides of these channels in SFM measurements look smoother and not at all vertical (see profile in Figure 1b) because of the finite tip radius of curvature (Figure 1c). From the triangle of Figure 1c we can deduce the tip radius:

$$R_t = \frac{w_m^2}{2h_m} + \frac{h_m}{2} \quad (2)$$

Here, w_m is the distance between the channel rim and the vertical tip radius and h_m is the depth of the channel measured from the relevant channel rim. These quantities can be accurately measured from corresponding SFM profiles taken perpendicular to the channels. A typical one is depicted in Figure 1b. Care has to be taken that the width of the channel is smaller than the expected diameter of the tip. Using channels in various directions, one can reconstruct the end of the tip quite accurately. In fact the *total* profile of the tip can be imaged as shown in the insert of Figure 1b. The black dots correspond to the measured tip profile (imaged at the sharp edge of the gold crystal) while the continuous line is an arc of a circle with a radius of 55 nm. Using this procedure we measured the tip radius (in four directions) for the measurements that we have performed under water. We found that the tip used was nearly spherical with an average radius of 55 nm. This compares with the manufacturer's estimate of 50 nm. The sizes of the polymer globules in SFM images were averaged from line profiles along (at least) four nonparallel directions across the globule image (the same directions used for the tip-radius estimation). Care has been taken to exclusively address polymer globules located in flat gold

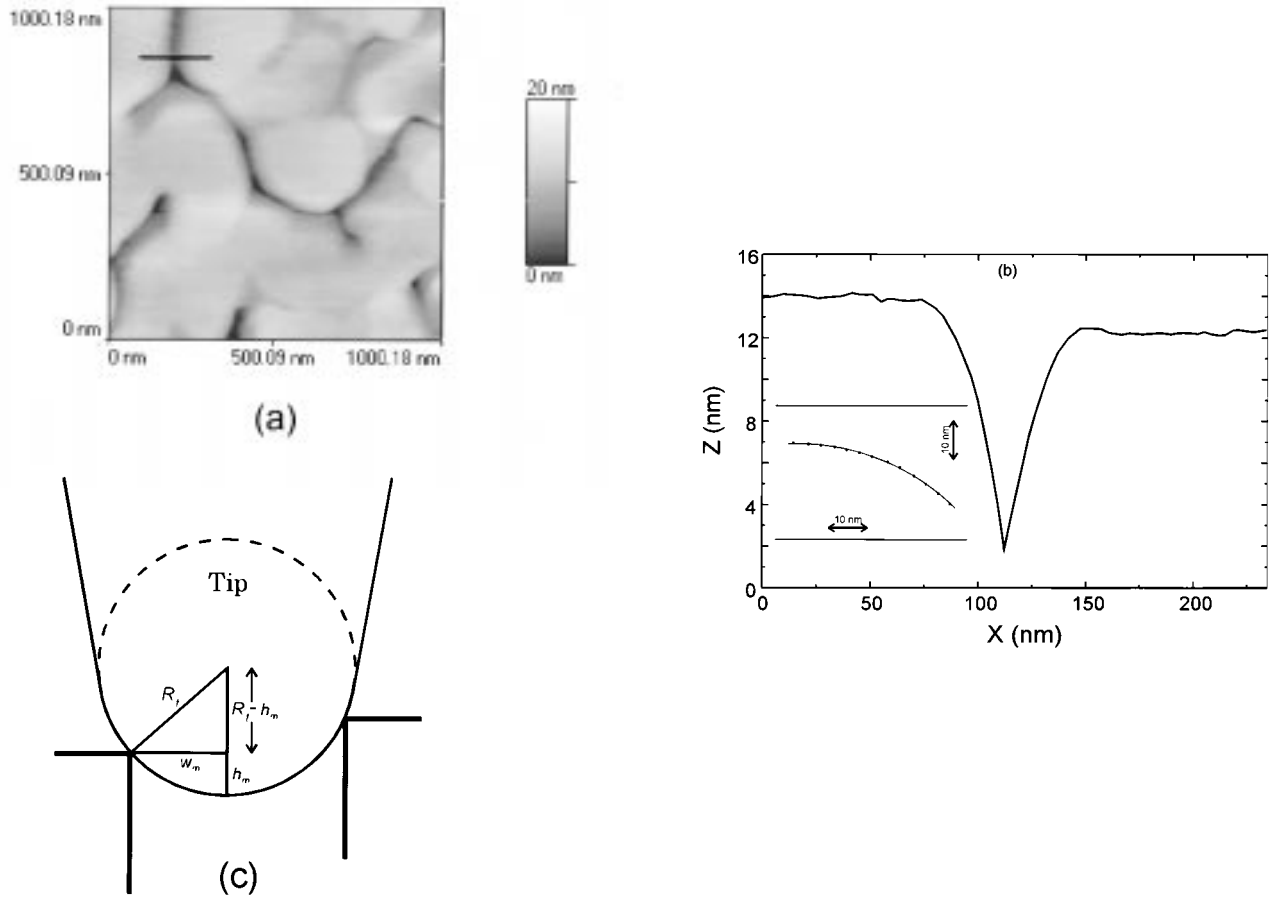

Figure 1. (a) SFM topography image of the bare gold surface obtained by evaporation of 40 nm of gold onto a freshly cleaved mica substrate. The black line indicates the trace of the profile of a channel between gold islands as it is imaged by SFM and shown in part b. The insert figure shows the fitting of the SFM profile (black dots) of the island's edge with a circle of 55 nm radius. The edge, being very sharp, images the tip apex. (c) Drawing showing the imaging process of a channel between gold islands by an SFM tip. Due to the finite tip radius, the depth of the channel is underestimated.

terraces and not near edges or channels, because in the latter case the tip convolution effects are more severe.

3. Results and Discussion

We have organized this section as follows. In the first subsection we show by XPS, ellipsometry, and SFM measurements that the polymer grafting density can be varied by changing the concentration of the alkanethiols in the solution. We proceed in the next subsection investigating the size of the polymer chains. In the last subsection we examine the lateral deformation of the chains and their frictional properties.

3.1. Varying the Polymer Grafting Density—Single Chains. From X-ray photoelectron spectroscopy, a sharp rise in the carbon-1s signal (C:Au ratio) is observed at a mole fraction of $\phi_{PS-SH} \approx 0.8-1.0$, indicating an increase in polymer adsorption at higher values of ϕ_{PS-SH} (Figure 2). The presence of polystyrene on the surface can be confirmed by the $\pi-\pi^*$ shake-up satellite at ϕ_{PS-SH} values higher than 0.8. The increase in polymer adsorption at sufficiently high ϕ_{PS-SH} values can be explained by a smaller diffusion coefficient for PS-SH compared to dodecanethiol and the fact that the polystyrene chain in an apolar solvent (toluene) will shield its polar thiol group. Compared to the dodecanethiol molecule, the thiol group in PS-SH therefore has a much lower probability to react with the gold surface. This results in a smaller mole fraction of chemisorbed PS-SH than would be expected from the

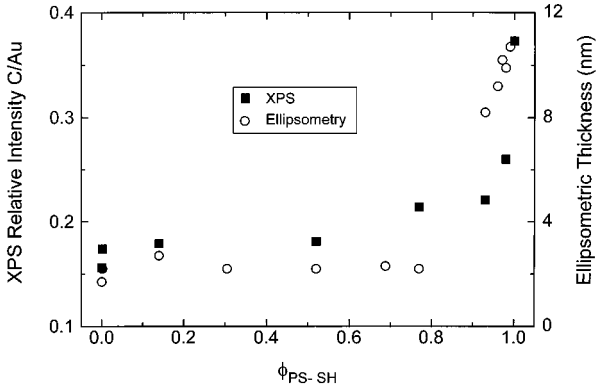

Figure 2. Relative peak intensity of the C_{1s}/Au_{4f} signal (filled squares) and ellipsometric thickness (hollow circles) for various mole fractions ϕ_{PS-SH} of PS_{400}-SH molecules.

mole fraction of PS-SH in the adsorption solution under the assumption that both molecules diffuse at the same rate. Ellipsometry measurements (Figure 2) verify that for values of ϕ_{PS-SH} above about 0.8 there is a considerable increase in the average thickness of the polymer layer.

In Figure 3 three SFM topography images of alkanethiol and PS_{400}-SH monolayers are shown, corresponding to different concentrations of alkanethiol in the adsorption solution and the same incubation time of 48 h. The images were obtained under ambient conditions. In Figure 3a, at a mole fraction of $\phi_{PS-SH} =$

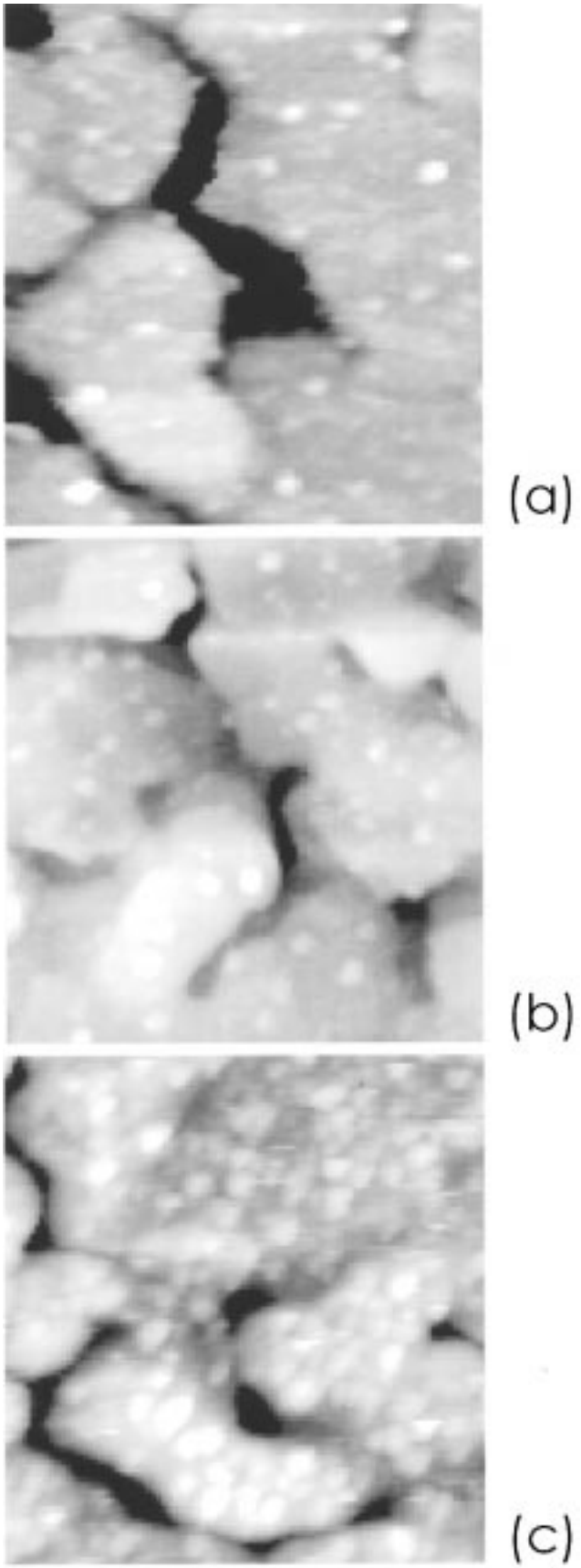

Figure 3. SFM topography images of the SAM corresponding to various mole fractions ϕ_{PS-SH} of the polymer ($M_w = 41\,500$) in the adsorbing solution: (a) $\phi_{PS-SH} = 0.77$, (b) $\phi_{PS-SH} = 0.84$, (c) $\phi_{PS-SH} = 0.98$. For all images, the black-to-white height difference equals 30 nm. The measurements were conducted under ambient conditions in the attractive regime.

0.77, individual polymer islands are observed (individual alkanethiols cannot be observed at this scale). As the mole fraction of the polymer in the solution is increased to $\phi_{PS-SH} = 0.84$, a higher density of polymer islands is detected (Figure 3b). When the polymer mole fraction is 0.98, the density of islands on the surface has increased accordingly (Figure 3c). The SFM images indicate the microscopic explanation for the average thickness increase that was observed in the ellipsometry measurements: the grafting density augments as the mole fraction of the polymer in the solution increases (Figure 2). SFM imaging was performed in the contact mode in the attractive regime. It was not possible to image the polymer islands in the repulsive regime under ambient conditions probably because of the meniscus forces (exerted by a water layer condensed on the sample) that can act as an additional load.[40,41] The lateral sizes of sample's structures may be greatly overestimated due to the convolution of the geometry of the tip and the sample. The molecular profiles in Figure 3c are broader than those presented in Figure 3a,b. This is due to the fact that the former have been measured using a Si_3N_4 tip which has an approximate end radius of 30−50 nm, while the latter have been measured using SiO_2 tips with an approximate end radius of 10−20 nm, thus appreciably reducing tip shape convolution effects. For the measurements taken with the Si_3N_4 tip, average values for the apparent height and width of the molecules are 3.9 and 33 nm, respectively. Assuming a half-sphere geometry for the individual polymer islands, one can calculate the radius of this half-sphere, from the molecular weight of the PS and its density. Using the bulk density of amorphous PS (1 g/cm^3), the radius is calculated to be about 3.2 nm, which is in reasonable agreement with the observed value of 3.9 nm. Hence, we conclude that the observed polymer islands are single collapsed chains. The observed variation in the shape of the islands in Figure 3 can be due to a variety of reasons: (1) dispersion in the molecular weight of the polymer, (2) variation in the deformation effects caused by a variation in the conformational state of the individual macromolecules; and (3) variation of the substrate corrugation around the collapsed chains (a particle on a peak will be imaged differently than a particle in a valley[9]).

In order to perform more accurate measurements which eliminate the unwanted compression that can result from meniscus forces or the possible coil pull-up in the attractive regime, we conducted SFM measurements under water where the applied external force can be more easily controlled.

3.2. Size and Volume of Single Chains. In Figures 4a,c and 5b,d we present the normal force (topography) and the lateral force images, respectively, of mixed monolayers of alkanethiol and PS-SH. Two molecular weights were used: PS_{1400}-SH (Figure 4a,b) and PS_{2500}-SH (Figure 4c,d). The mole fractions and concentrations in the solution were the same for both polymers (c = 1 mg/mL and $\phi_{PS_{1400}-SH} = \phi_{PS_{2500}-SH} = 0.85$). The images have been taken simultaneously under water with an applied load of about 1.0 nN. The PS_{1400}-SH polymer is more densely distributed since its molar concentration in the solution was larger in comparison with the molar concentration of PS_{2500}-SH. The polymer islands are clearly imaged, although some of them seem to be deformed and/or partially smeared out. Nevertheless, the majority of the single coils have

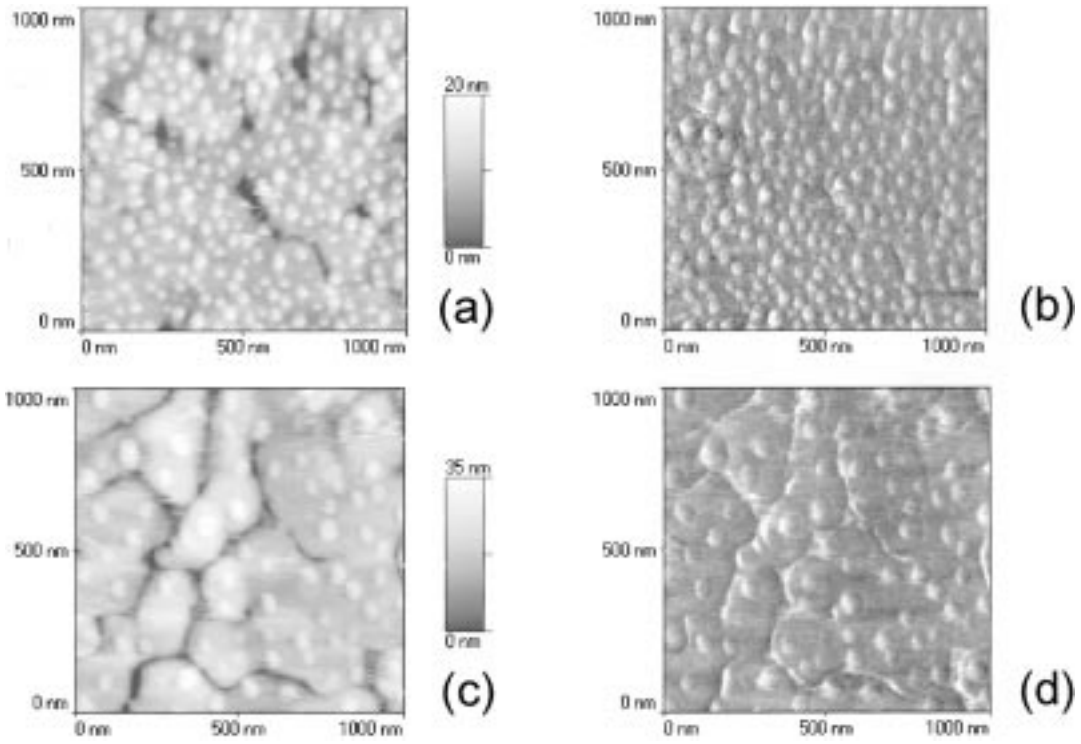

Figure 4. Topographic (a, c) and simultaneously acquired lateral force images (b, d) of a mixed monolayer of alkanethiol and PS-SH. (a, b) $PS_{1400}-SH$, $\phi_{PS_{1400}-SH} = 0.85$, $c = 1$ mg/mL and (c, d) $PS_{2500}-SH$, $\phi_{PS_{2500}-SH} = 0.85$, $c = 1$ mg/mL. For the lateral force images, bright/dark appearance indicates high/low lateral force.

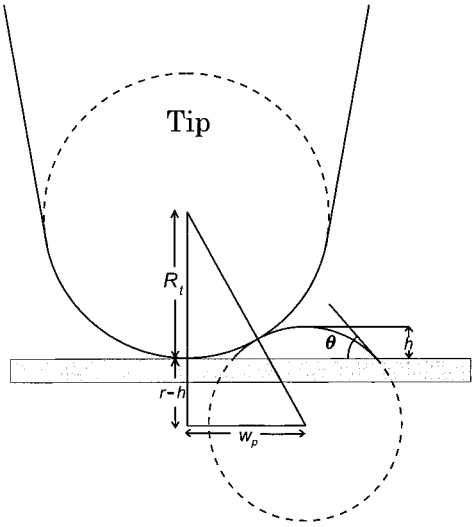

Figure 5. Drawing showing a spherical cap of radius r forming a contact angle θ with the substrate scanned by a tip of radius R_t. h and w_p are the measured height and (apparent) half-width of the spherical cap, respectively. When the substrate is flat, the height is measured correctly, but the width is overestimated.

apparently been subjected to only a slight deformation or none at all and we will concentrate now on their size and shape.

Since we used an applied load of 1 nN, we expect that the rather compliant sample[42] (Young's moduli: $E_{Au} =$ 80 GPa; $E_{PS} = 4$ GPa) will be indented by the stiff tip ($E_{Si_3N_4} = 130-150$ GPa). It is essential to see if there is any difference in the penetration depth for the two materials (Au + SAM and PS globules) since this could affect the measured heights in topography images. On the basis of contact mechanics[43] we evaluated the magnitude of this effect. Applying JKRS theory,[44] the penetration depth was found to be about 0.2 nm for the PS globules and 0.1 nm for gold. The heights of the polymer islands are in the range of 5−10 nm. Hence, the error in heights from this reason is about 1−2%, which is small and was neglected.

If we consider the shape of a polymer island to be close to a spherical cap (the treatment of small globules in terms of macroscopic quantities is justified even for single collapsed polymer coils; for details see ref 45), we can estimate its radius (r) (eq 3) and contact angle (θ) (eq 4) in terms of its apparent width (w_p), height (h) and tip radius (R_t) Figure 5:

$$r = \frac{w_p^2}{2h} + \frac{h}{2} - R_t \tag{3}$$

$$\cos\theta = 1 - \frac{h}{r} \tag{4}$$

Knowing the radius and the contact angle of the polymer cap, its volume can be calculated:

$$V_c = \frac{1}{3}\pi r^3(1 - \cos\theta)^2(2 + \cos\theta) \tag{5}$$

We measured the half-width (w_p) and the height (h) of the collapsed chains from corresponding line profiles (Figure 6). We considered polymer coils that (1) are well on the flat gold terraces, since polymer images close to edges suffer from artefacts that are not easy to deal with and (2) not heavily deformed. The radii r, the angles θ and the volumes V_c of the polymer islands were calculated from the measured quantities w_p and h via the above equations for each island separately. Taking the density of a collapsed PS chain as approximately equal to the usual bulk polystyrene density, we estimated its volume (V_t) from its molecular weight. In Table 2 we

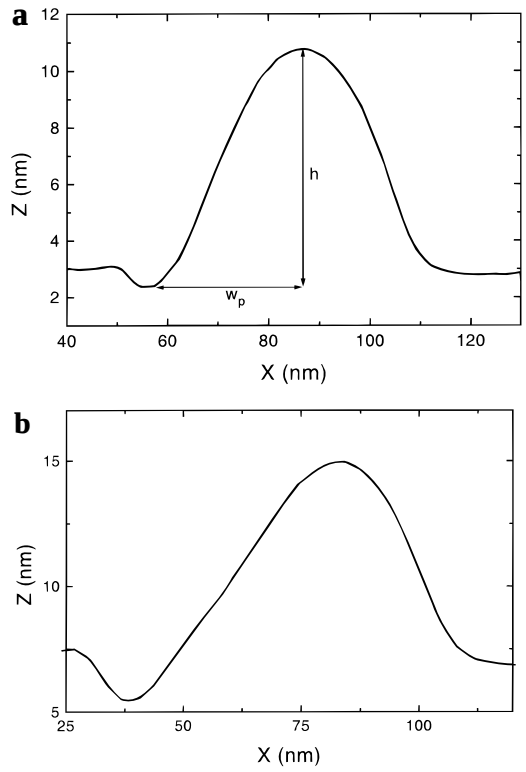

Figure 6. Cross-profile of (a) an undeformed and (b) a deformed and/or dragged PS_{2500}-SH molecule.

Table 2. Measured and Calculated Average Values for Collapsed Polymer Coils

polymer	h^a (nm)	$w_p{}^a$ (nm)	r^b (nm)	θ^b (deg)	$V_c{}^b$ (nm^3)	$V_t{}^c$ (nm^3)
PS_{1400}-SH	6.2	26.5	4.7	110 ± 15	320 ± 95	239
PS_{2500}-SH	8.9	31.7	5.9	115 ± 15	678 ± 210	428

[a] Measured values from SFM images. [b] Calculated values based on SFM images. [c] Estimated values based on the assumption that the polymer density is 1 g/cm^3.

summarize the average measured quantities w_p and h; the average calculated ones r, θ, and V_c; and the theoretically estimated volumes V_t. We can see that the calculated volumes V_c of the polymer islands are in the range of the theoretically predicted V_t values. However, V_c exceeds V_t by 30%. This can be tentatively attributed to some toluene molecules that were trapped during the collapse of the coil. Some polymer islands occupy volumes close to the volumes that two chains, collapsed together, would occupy. Consequently, we cannot entirely exclude the presence of some polymer islands consisting of two chains.

3.3. Lateral Deformation of Single Chains and Their Frictional Behavior. In the profile of Figure 6a we can see a small trough *just before* the tip encounters the chain (direction of scanning from left to right). The appearance of the trough is more prominent and more clearly visible for PS_{2500}-SH than for lower molecular weights.

In Figure 6b a typical profile of a deformed collapsed chain is shown. We see that the size of the trough is larger and that the polymer island is pulled by the tip in the direction of scannings, making its shape asymmetric (the slope on the left is less steep than the slope on the right). The average depth of the trough for the PS_{2500}-SH molecules is about 2 nm and its lateral size (in the direction of scanning along the diameter of the chain) varies from about 5−15 nm. For the PS_{1400}-SH molecules the trough appears only rarely with depth and lateral size of about 1 and 5 nm, respectively. This feature is totally absent when PS-SH is chemisorbed on a bare gold substrate from solutions that do not contain alkanethiols.[9] On the basis of these observations and on the fact that the height of the dodecanethiol SAM is about 2 nm we associate the appearance of the trough with the area around the grafted chains, unfilled (or partially filled) with dodecanethiols. Because of the unfavourable interactions between the grafted chains and the alkanethiols in the solution, we expect a reduced chemisorption of alkanethiols in the vicinity of the grafted coils: in a way, the swollen polymer coil "masks" its neighborhood (Figure 7a). When the polymer collapses (Figure 7b) its size decreases, and because of the presence of the alkanethiol layer around it, a trough forms. This trough is inaccessible to the tip because the tip radius is much larger. However, it can be imaged, from one side only, when the polymer chain is dragged and/or deformed by the tip in the direction of scanning. In this case, the collapsed chain is pulled over some nanometers by the tip, partially exposing the bare area in the vicinity of the single globule (Figure 7c). The dragging and/or deformation of the collapsed polymer chains can be explained partly by the nonideal force control on impact and partly by the larger friction coefficient of PS relatively to that of the alkanethiol SAM. When the tip encounters the polymer, it is transferred from a low-friction region (alkanethiol) to

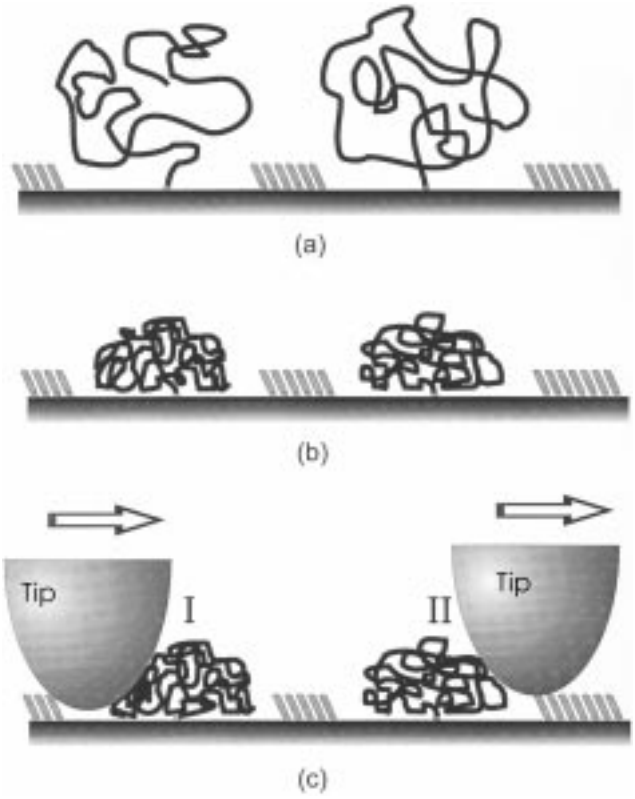

Figure 7. Schematic drawing of a mixed monolayer: a in solution (a) under good-solvent conditions the polymer coil is expanded (swollen) and prevents the alkanethiol molecules from adsorbing in its vicinity, (b) under bad-solvent conditions, the polymer chains collapse on the surface leaving an empty area around them. (c) The imaging process: (I) the polymer globule is dragged and/or deformed by the tip and the widened trough is imaged, and (II) due to convolution the trough is not imaged.

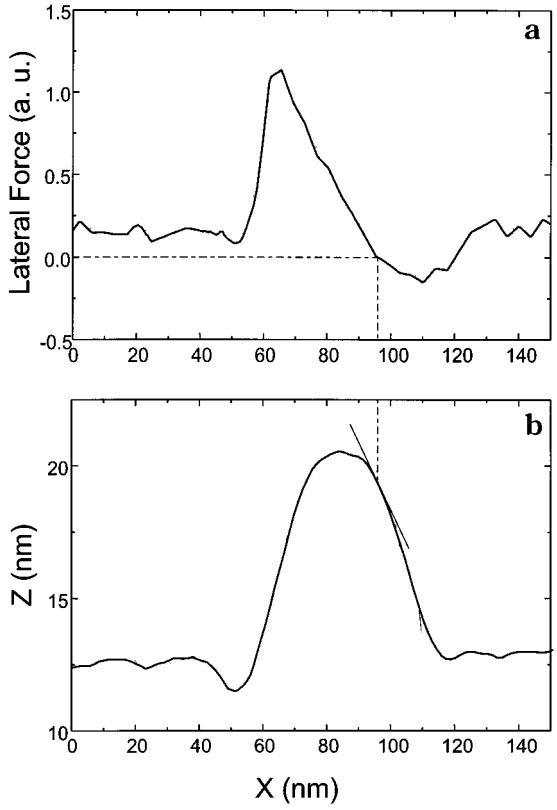

Figure 8. Simultaneously obtained cross-profiles along a single polymer chain: lateral force (a) and topography (b). At the first point of zero total lateral force (zero torsion) the corresponding negative slope of the topography is equal to the coefficient of friction μ.

a high-friction one (polymer). Thus, either (a) the tip sticks to the polymer and drags it for a short period until the resistance of the polymer via the tether is high enough for the tip to slide and proceed over it, (b) the tip deforms the polymer globule elastically in the direction of scanning due to relatively high friction on the polymer chain (actually, this effect has been observed in simulations by Aimé et al.[46]), or (c) both effects occur. The friction coefficient of CH_3-terminated SAM's has been measured with SFM to be around 0.02−0.05.[47] The macroscopic friction coefficient of amorphous PS is 0.515,[48] but it would be more relevant to measure the local friction coefficient on the polymer globules. This can be accomplished by addressing lateral force profiles and topography profiles obtained simultaneously.

In Figure 8 we present a lateral force profile (a) and the corresponding, simultaneously taken topographical one (b) of a single collapsed chain. The frictional force resembles the first derivative of topography (dz/dx). Haugstad et al.[49] showed that the total torque τ that is exerted on the cantilever is given by[50]

$$\tau \approx F_l L\left(\frac{\mathrm{d}z}{\mathrm{d}x} + \mu\right) \qquad (6)$$

where F_l is the applied normal load, which remains constant, L is the distance between the principal cantilever axis and the vertex of the spherical tip, and μ is the local coefficient of friction. dz/dx is evaluated at the point of contact. This model explains why the frictional signal varies as the first derivative of topography. It follows from eq 6 that at the point where τ vanishes the coefficient of friction is equal to the negative slope of the topography. This is actually happening once during the descent of the tip from the polymer coil, at the point where the slope is −0.26; hence $\mu = 0.26$. Using this method, we measured the local friction coefficient for several single collapsed chains: we found an average value of about 0.3, which is in the range of the macroscopic value.

To our knowledge this is the first report of the local friction coefficient on a single polymer chain. This relatively high friction coefficient, compared with the friction coefficient of the alkanethiol SAM, can account for the deformation and/or dragging of the single polymer globules in the direction of scanning.

4. Conclusions

The spontaneous adsorption of PS-SH molecules and alkanethiols onto Au surfaces from mixed solutions in toluene resulted in an adsorbate containing isolated polymer chains randomly distributed in a SAM of alkanethiols. We showed that the grafting density of the chains can be changed by varying the molar ratio of the components in the solution. The majority of the collapsed chains exhibited structural stability, although some of them were deformed and/or dragged by the tip during imaging. This effect can be attributed partly to the topographical change and partly to the high local friction coefficient of single PS globules, which was measured to be in the range of that of bulk polystyrene.

Acknowledgment. We would like to thank Dr. M. A. C. Devillers (Exp. Solid State Physics, University of Nijmegen) for the ellipsometry measurements, A. Stamouli for the light scattering measurements, Dr. E. Pelletier for useful discussions, and Dr. Paul van Hutten for the careful reading of the manuscript. This work was supported by the Netherlands Foundation for Fundamental Research on Matter (FOM) and the Netherlands Organization for Scientific Research (NWO).

References and Notes

(1) Napper, D. *Polymeric Stabilization of colloidal Dispersions*, Academic Press: London, 1983.
(2) Pludeman, E.; Collins, N. *Adhesion Science and Technology*, Plenum Press: New York, 1975; Vol. 9a.
(3) De Gennes, P. G. *J. Phys.* (Fr.) **1989**, *50*, 2551.
(4) Brown, H. R. *Science* **1994**, *263*, 1411.
(5) Migler, K.; Hervet, H.; Léger, L. *Phys. Rev. Lett.* **1993**, *70*, 287.
(6) Milner S. T. *Science* **1991**, *251*, 905.
(7) Zhao, W.; Krausch, G.; Rafailovich, M. H.; Sokolov, J. *Macromolecules* **1994**, *27*, 2933.
(8) Siqueira, D. F.; Köhler, K.; Stamm M. *Langmuir* **1995**, *11*, 3092.
(9) Koutsos, V.; van der Vegte, E. W.; Pelletier, E.; Stamouli, A.; Hadziioannou, G. *Macromolecules* **1997**, *30*, 4719.
(10) Ulman, A. *An Introduction to Ultrathin Organic Films*, Academic Press: San Diego, CA, 1991.
(11) Porter, M. D.; Bright, T. B.; Allara, D. L.; Chidsey, C. E. D. *J. Am. Chem. Soc.* **1987**, *109*, 3559.
(12) Bain, C. D.; Troughton, E. B.; Tao, Y.-T.; Evall, J.; Whitesides, G. M.; Nuzzo, R. G. *J. Am. Chem. Soc.* **1989**, *11*, 321.
(13) Nuzzo, R. G.; Dubois, L. H.; Allara, D. L. *J. Am. Chem. Soc.* **1990**, *112*, 558.
(14) Dubois, L. H.; Zegarski, B. R.; Nuzzo, R. G. *J. Am. Chem. Soc.* **1990**, *112*, 570.
(15) Laibinis, P. E.; Fox, M. A.; Folkers, J. P.; Whitesides, G. M. *Langmuir* **1991**, *7*, 3167.
(16) Bertilsson, L.; Liedberg, B. *Langmuir* **1993**, 9, 141.
(17) Grunze, M. *Phys. Scripta* **1993**, *T49*, 711.
(18) Kim, Y.-T.; McCarley, R. L.; Bard, A. J. *J. Phys. Chem.* **1992**, *96*, 7416.
(19) McCarley, R. L.; Kim, Y.-T.; Bard, A. J. *J. Phys. Chem.* **1993**, *97*, 211.

(20) Widrig, C. A.; Alves, C. A.; Porter, M. D. *J. Am. Chem. Soc.* **1991**, *113*, 2805.
(21) Alves, C. A.; Smith, E. L.; Porter, M. D. *J. Am. Chem. Soc.* **1992**, *114*, 1222.
(22) Zak, J.; Yuan, H.; Ho, M.; Woo, L. K.; Porter, M. D. *Langmuir* **1993**, *9*, 2772.
(23) Caldwell, W. B.; Chen, K.; Mirkin, C. A.; Babinec, S. J. *Langmuir* **1993**, *9*, 1945.
(24) Sabatani, E; Cohen-Boulakia, J.; Bruening, M.; Rubinstein, I. *Langmuir* **1993**, *9*, 2974.
(25) Häussling, L.; Ringsdorf, H.; Schmitt, F.-J.; Knoll, W. *Langmuir* **1991**, *7*, 1837.
(26) Spinke, J.; Liley, M.; Schmitt, F,-J.; Guder, H.-J.; Angermaier, L.; Knoll, W. *J. Chem. Phys.* **1993**, *99*, 7012.
(27) Lang, H.; Duschl, C.; Vogel, H. *Langmuir* **1994**, *10*, 197.
(28) Niwa, H.; Shimoguphi, M.; Higashi, N. *J. Colloid Interface Sci.* **1992**, *148*, 592.
(29) Stouffer, J. M.; McCarthy, T. J. *Macromolecules* **1988**, *21*, 1204.
(30) Sun, F.; Castner, D. G.; Grainger, D. W. *Langmuir* **1993**, *9*, 3200.
(31) Whitesell, J. K.; Chang, H. K. *Science* **1993**, *261*, 73.
(32) O'Shea S. J.; Welland, M. E.; Rayment T. *Langmuir* **1993**, *9*, 1826.
(33) Stamouli. A.; Pelletier, E.; Koutsos, V.; v.d. Vegte E. W.; Hadziioannou G. *Langmuir* **1996**, *12*, 3221.
(34) Akari, S.; v.d. Vegte, E. W.; Grim, P. C. M.; Belder, G. F.; Koutsos, V.; ten Brinke, G.; Hadziioannou, G. *Appl. Phys. Lett.* **1994**, *65*, 1915.
(35) Tang, W. T. *Study of block copolymer micelles in dilute solution by light scattering and fluorescence spectroscopy*; dissertation, Stanford University, 1987, p 28−33.
(36) de Gennes, P.-G. *Scaling Concepts in Polymer Physics*; Cornell University Press: Ithaca, NY, 1979.
(37) (a) Shimazu, K.; Yag, I.; Sato, Y; Uosaki, K. *Langmuir* **1992**, *8*, 1385. (b) Karpovich, D. S.; Blanchard, G. J. *Langmuir* **1994**, *10*, 3315. (c) Grunze, M. *Phys. Scripta* **1993**, *T49*, 711.
(38) Binnig, G.; Quate, C. F.; Gerber, Ch. *Phys. Rev. Lett.* **1986**, *56*, 930.
(39) Zheng, X.-Y.; Youzhen D.; Bottomley, L. A. *J. Vac. Sci. Technol.* **1995**, *B13(3)*, 1320.
(40) Weisenhorn, A. L.; Hansma, P. K.; Albrecht, T. R.; Quate, C. F. *Appl. Phys. Lett.* **1989**, *54*, 2651.
(41) Burnham, N. A.; Colton, R. J.; Pollok H. M. *J. Vac. Sci. Technol.* **1991**, *A9*, 2548.
(42) We assume that SAM's do not change significantly the elastic behavior of solids. For example, see: Thomas, R. S.; Houston, J. E.; Michalske T. A.; Crooks, R. M. *Science* **1993**, *259*, 1883.
(43) (a) Johnson K. L. *Contact Mechanics*; Cambridge University Press: Cambridge, 1985. (b) Horn, R. G.; Israelachvili J. N.; Pribac F. *J. Colloid Interface Sci.* **1987**, *115(2)*, 480.
(44) (a) Johnson, K. L.; Kendal K.; Roberts A. D. *Proc. R. Soc. London A* **1971**, *324*, 301. (b) Sperling, G. Ph.D. Thesis in Karlsrule Technical High School, 1964.
(45) Johner, A.; Joanny J. F. *J. Phys. II* **1991**, *1*, 181.
(46) Aimé J. P.; Elkaakour, Z; Gauthier S.; Michel D.; Bouhacina T.; Curély J. *Surf. Sci.* **1995**, *329*, 149.
(47) Tsukruk, V. V.; Everson, M. P.; Lander, L. M.; Brittain, W. J. *Langmuir* **1996**, *12*, 3905.
(48) *Polymer Handbook*, 3rd ed.; Brandrup, J., Immergut, E. H., Eds.; Wiley: New York, 1989.
(49) Haugstad, G.; Gladfelter, W. L. *Langmuir* **1993**, *9*, 3717.
(50) This model applies only if the factor $R_t/L[1 + (dz/dx)^2]^{1/2}$ is sufficiently small (≤0.1). This holds since $R_t/L \approx 0.02$ and $dz/dx \leq 5$.

MA9706182